Endovascular biopsy: Strategy for analyzing gene expression profiles of individual endothelial cells obtained from human vessels[☆]

Zhengda Sun[a], Devon A. Lawson[b], Elizabeth Sinclair[c], Chih-Yang Wang[b,e], Ming-Derg Lai[e], Steven W. Hetts[a], Randall T. Higashida[a], Christopher F. Dowd[a], Van V. Halbach[a], Zena Werb[b], Hua Su[d,1], Daniel L. Cooke[a,1,*]

[a] Division of Neurointerventional Radiology, Department of Radiology and Biomedical Imaging, University of California, San Francisco, CA, USA
[b] Department of Anatomy, University of California, San Francisco, CA, USA
[c] Division of Experimental Medicine, Department of Medicine, University of California, San Francisco, CA, USA
[d] Center for Cerebrovascular Research, Department of Anesthesia and Perioperative Care, University of California, San Francisco, CA, USA
[e] Department of Biochemistry and Molecular Biology, Institute of Basic Medical Sciences, College of Medicine, National Cheng Kung University, Tainan, Taiwan

ARTICLE INFO

ABSTRACT

Purpose: To develop a strategy of achieving targeted collection of endothelial cells (ECs) by endovascular methods and analyzing the gene expression profiles of collected single ECs.
Methods and results: 134 ECs and 37 leukocytes were collected from four patients' intra-iliac artery endovascular guide wires by fluorescence activated cell sorting (FACS) and analyzed by single-cell quantitative RT-PCR for expression profile of 48 genes. Compared to CD45^{+} leukocytes, the ECs expressed higher levels ($p < 0.05$) of EC surface markers used on FACS and other EC related genes. The gene expression profile showed that these isolated ECs fell into two clusters, A and B, that differentially expressed 19 genes related to angiogenesis, inflammation and extracellular matrix remodeling, with cluster B ECs have demonstrating similarities to senescent or aging ECs.
Conclusion: Combination of endovascular device sampling, FACS and single-cell quantitative RT-PCR is a feasible method for analyzing EC gene expression profile in vascular lesions.

1. Introduction

Gene expression studies of patient-derived endothelial cells (ECs) provide important information regarding the pathogenesis of many vascular diseases [1–3], in and outside of the central nervous system. Several groups have reported EC enrichment and identification from endovascular guide wires by 2 EC separation methods: micropipette picking-up [4] or CD146 antibody-conjugated magnetic beads [5–7], both followed by either traditional gene expression assays like bulk mRNA reverse transcription (RT) PCR which analyzes RNA extracted from a pool of ECs [4,5], quantitative RT-PCR [6] or quantitative immunofluorescence [7–

14]. Because of the limitation set by these conventional methods, only a few (up to 3 or 4) genes can be analyzed. Due to the complexity and heterogeneity of ECs [15], these studies have incurred uncertainty and controversy regarding the purity and functionality of the ECs studied.

Although DNA microarray studies of ECs separated from tissue can provide high throughput EC gene expression information and have indicated that heterogeneity of endothelium exists among different tissues or diseases [15,16], this technique needs bulk mRNA extracted from at least thousands of ECs, numbers difficult to attain using endovascular EC sampling methods. Furthermore, DNA microarray can only analyze gene expression patterns of a group of ECs and not each individual EC. A more complete picture of individual EC functional condition in specific environments needs an assay, which can analyze the expression profile of multiple genes in individual ECs.

Recently we reported that EC candidates attached on guide wires can be collected by fluorescence activated cell sorting (FACS) and laser capture microdissection. The quality of mRNA extracted from the ECs is sufficient for analysis of gene expression using quantitative RT-PCR [17]. Single-cell quantitative RT-PCR

* Corresponding author at: Interventional Neuroradiology, 505 Parnassus Avenue, Box-0628, San Francisco, CA 94143, USA. Fax: +1 415 353 8606.
E-mail address: cooke@ucsf.edu (D.L. Cooke).
[1] Co-senior authors.

combined with high-throughput microfluidic array technology facilitates detection of gene expression profiles of up to 96 genes in 96 individual cells simultaneously [18,19]. Therefore, it is a powerful high throughput tool to characterize gene expression of individual cells.

In this study, we demonstrated that combination of FACS and high throughput microfluidic single-cell quantitative RT-PCR is an efficient and powerful method for analyzing the changes of EC gene expression profiles in vascular lesions.

2. Material and methods

2.1. Case selection and EC harvest

Samples were collected from four patients undergoing routine catheter angiography for assessment of cerebrovascular pathology. The patients provided written consent for the procedure inclusive of the collection and study of tissues for research purposes standard on surgical consent forms. ECs were obtained by inserting a 0.038-inch diameter coaxial curved stainless steel guide wire (Cook Inc., Bloomington, IN) into the right iliac artery as part of routine arterial access. Wires are directed under fluoroscopic visualization so a short (<5 cm) segment of vessel may be specifically contacted. The cells attached on the wires were dislodged by vortexing and centrifuging in a dissociation buffer (Gibco, Grand Island, NY). After lysing RBC by ACK Lysing Buffer (Gibco, Grand Island, NY), and centrifuged at 1500 rpm, the pellets were re-suspended in FACS buffer for incubation of antibodies and sorting. Experiment design is shown in Fig. 1.

2.2. EC candidate identification and sorting on FACS

Single EC candidates were identified and sorted by a protocol of seven fluorescently-conjugated monoclonal antibodies on FACS that we described in our previous study [17]. LIVE/DEAD Fixable Dead Cell Stain (Life Technologies, Carlsbad, CA) was used to exclude the dead cells. The antibody information is listed in Table 1.

Table 1
Fluorescently conjugated monoclonal antibodies used for EC candidate identification on FACS.

Target	Format	Dilution	Vendor	Catalog number
CD31	Alexa 647	1:500	BD Biosciences	561654
CD34	PE-Cy7	1:50	Biolegend	343516
CD105	PE-CF594	1:100	BD Biosciences	562380
CD146	PE	1:50	BD Biosciences	561013
CD45	Alexa 700	1:50	Life technologies	MHCD4529
CD11b	PacBlue	1:50	Biolegend	301324
CD42b	FITC	1:50	BD biosciences	555472

After staining the dislodged cells with these seven antibodies and the Amine Aqua Reactive Dye (AmCyan channel), the debris, doublets and dead cells were excluded before subsequent procedures (Fig. 2). After excluding CD45$^+$ leucocytes, CD11b$^+$ myeloid cells and CD42b$^+$ platelets by three negative gates, the remaining cells were gated by four EC specific surface markers, CD31, CD34, CD105 and CD146. Cells positive for the 4 EC surface markers were collected as EC candidates. CD45$^+$ leucocytes were also collected and used as control. EC candidates and leukocytes were sorted into 96 well plates on a FACS Aria II (BD Biosciences, San Jose, CA) with 100 nm nozzle using single cell sort mode.

2.3. Reverse Transcription and cDNA pre-amplification

Reverse transcription and cDNA pre-amplification were carried out on a PCR thermocycler. Briefly, each EC candidate was sorted directly into one well with 9 μL reverse transcription-specific target amplification (RT-STA) buffer on the 96-well plates (Eppendoff, Hauppauge, NY). The RT-STA buffer contained 5 μL CellsDirect 2× Reaction Mix (Life Technologies, Carlsbad, CA), 0.2 μL SuperScript III RT Platinum Taq Mix (Life Technologies, Carlsbad, CA), 2.8 μL nuclease free water and 1 μL 10× primer mixture (500 nM) that contained a mix of 48 pairs of primers specific to genes listed in Table 2. The primers were custom designed and all expand introns to minimize the genomic DNA
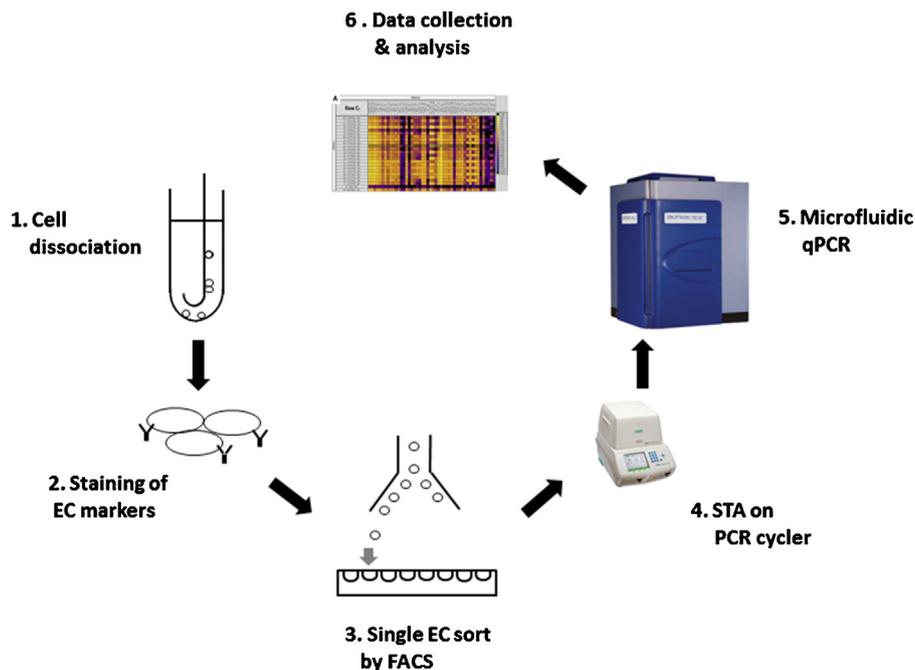

Fig. 1. Experimental design. Cells were dislodged from the guide wire (1) and were stained by antibodies specific for different cell surface markers (2). Individual ECs were sorted into 96-well plates by FACS (3). Specific gene cDNAs were pre-amplified by thermocycler (4). Quantitative RT-PCR was performed on Biomark HD system (Fluidigm, South San Francisco, CA) (5). Data were collected and analyzed by quantitative RT-PCR analysis software (Fluidigm, South San Francisco, CA) (6).
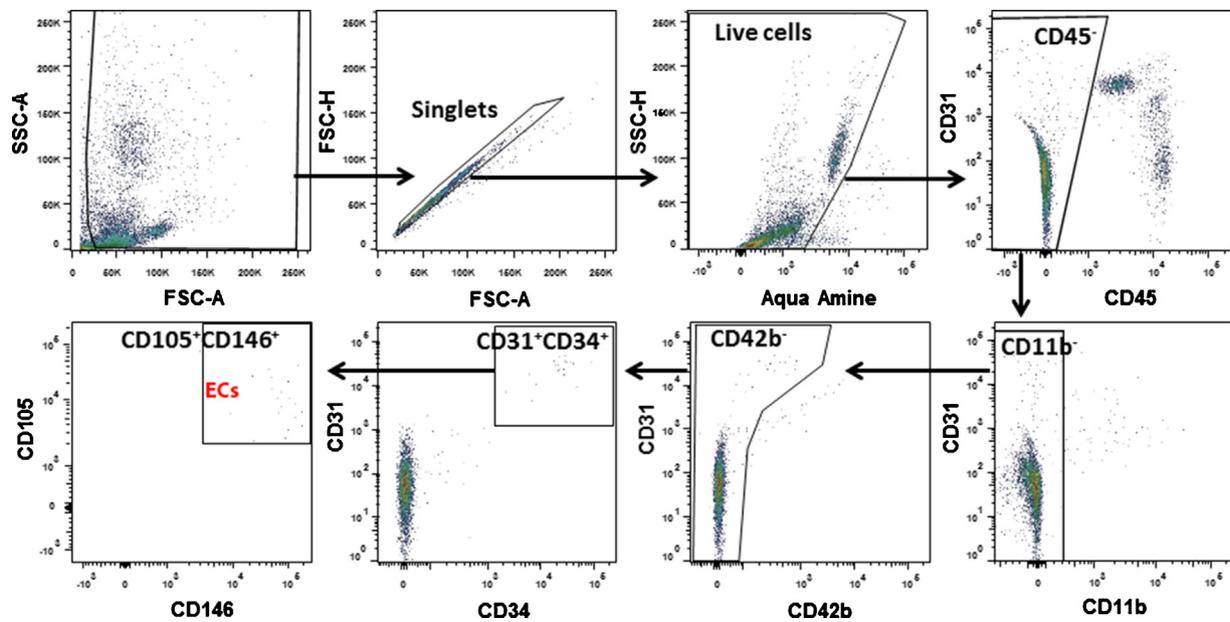
Fig. 2. FACS gating strategy for EC collection. Seven cell surface markers and one viability marker were used to gate the EC candidates. Cells were first gated to exclude debris, doublets and dead cells identified by positive Aqua Amine stain. After gating on the viable single cells, the leukocytes (CD45$^+$), macrophages (CD11b$^+$) and platelets (CD42b$^+$) were eliminated. EC candidates were first selected by CD31 and CD34, and then CD105 and CD146.

fraction (Fluidigm, South San Francisco, CA). The Fluidigm Assay IDs listed in Table 2 can be used to obtain primer sequences.

The samples were incubated at 50 °C for 15 min for the reverse transcription, 95 °C for 2 min for inactivating reverse transcriptase and activating Taq polymerase, then subjected to 18 PCR cycles (95 °C 15 sec then 60 °C for 4 min for each cycle) for specific targets amplification (STA). To remove the unincorporated primers for best results, each sample was then mixed with 3.6 μL exonuclease treatment buffer composed of 2.52 μL water, 0.36 μL 10× Exonuclease I reaction buffer and 0.72 μL 20 units/ μL Exonuclease I (New England BioLabs, Ipswich, MA), incubated at 37 °C for 30 min for digestion and 80 °C for 15 min to inactivate the exonuclease.

2.4. Quantitative RT-PCR

48.48 nanofluidic chips and a BioMark HD system (Fluidigm, South San Francisco, CA) were used. Briefly, each pre-amplified cDNA sample was diluted by 5 fold in TE Buffer (TEKnova, Hollister, CA). Then, 2.25 μL diluted samples were mixed with 2.5 μL 2x SsoFast EvaGreen Supermix with Low ROX (Bio-Rad, Hercules, CA) and 0.25 μL 20× DNA Binding Dye Sample Loading Reagent (Fluidigm, South San Francisco, CA). The pre-mix samples (5 μL each) were loaded into the 48 sample inlets on the 48.48 Dynamic Array (Fluidigm, South San Francisco, CA), which had been primed with control line fluid (Fluidigm, South San Francisco, CA) on IFC Controller MX (Fluidigm, South San Francisco, CA). Assay Mix (5 μl) containing 2.5 μL 2× Assay Loading Reagent (Fluidigm, South San Francisco, CA), 2.25 μL 1× DNA suspension buffer (TEKnova, Hollister, CA) and 0.25 μL primer set (100 μM) were added to the 48 assay inlets on the 48.48 nanofluidic chip (Fluidigm, South San Francisco, CA). After loading both pre-mixed samples and the assay mixtures to the nanochip by IFC Controller MX (Fluidigm, South San Francisco, CA), the chip was loaded into the BioMark HD system (Fluidigm, South San Francisco, CA) for PCR through 35 cycles of 5 sec at 96 °C and 20 sec at 60 °C after a hot start phase of 60 sec at 95 °C. Fluorescence in the EvaGreen channel was detected and collected by a CCD camera placed above the chip and 6-carboxy-X-rhodamine (ROX) intensity was used as normalization.

2.5. Data collection and analysis

Quantitative RT-PCR data of ECs and leukocytes obtained from 4 subjects were analyzed together. Fluidigm quantitative RT-PCR Analysis software (Fluidigm, South San Francisco, CA) was used to process RT-PCR data obtained by Biomark HD system and calculate Ct values. Ct values were further processed in the R statistical language using algorithms provided by SINGuLAR Analysis Toolset 3.5 (Fluidigm, South San Francisco, CA). All Raw Ct values were normalized to the assumed detection Ct level of 24 following the recommendation from this manual. Ct values were converted to relative expression levels using methods described previously [20]. The assumed minimum value of genes without expression was set as 10% lower than the lowest recorded reading. Euclidean distance metric and complete linkage function were used to build the Hierarchical clustering. Mean-centered data were used for principal components analysis (PCA) to avoid bias caused by highly expressed genes.

3. Results

3.1. Selection of genes for profiling EC gene expression

Based on previous EC function studies [21,22], we selected three groups of genes to characterize ECs in this study. They are 19 angiogenesis-related genes, 13 inflammation-related genes and 12 extra-cellular matrix (ECM) remodeling-related genes. To confirm the identity of ECs isolated by FACS, six EC specific marker genes and one vascular smooth muscle cell marker gene (α-actin) were included. We also included the four EC-marker genes and CD45 that were used for FACS selection of EC candidates and leukocytes (Table 2).

3.2. The gene expression profile of EC candidates is distinctively different from that of LCs

A total of 134 EC candidates and 37 leukocytes (LCs) were collected by FACS through the gating strategy we described previously [17] and shown in Fig. 2. Among these ECs, 64 (48%)

Table 2
Genes selected for single gene expression analysis.

Gene group	Symbol	Gene name	Description	Function and reference	Fluidigm assay ID[b]
Cell marker	PTPRC[a]	CD45	Protein tyrosine phosphatase, receptor type C	Leucocyte marker	GEP00055840
	PECAM1[a]	CD31	platelet endothelial cell adhesion molecule-1	Adhesion molecular, inflammation [32]	GEP00056436
	CD34[a]	CD34	Hematopoietic Progenitor Cell Antigen	EC marker, inflammation [33]	GEA00011907
	ENG[a]	CD105	Endoglin	EC marker, angiogenesis [34]	GEP00056632
	MCAM[a]	CD146	Melanoma cell adhesion molecule	EC marker, inflammation [35–38]	GEP00056760
	KDR	Flk1	vascular endothelial growth factor receptor 2	EC marker, angiogenesis [39,40]	GEA00012361
	FLT1	VEGFR1	vascular endothelial growth factor receptor 1	EC marker, migration [41]	GEP00055864
	TIE1	Tie1	tyrosine kinase with Ig-like and EGF-like domains 1	EC marker, Angiogenesis [39,42]	GEA00012787
	THBD	–	Thrombomodulin	EC marker [43]	GEA00014984
	VWF	vWF	Von Willebrand factor	EC marker, angiogenesis [44]	GEA00013832
	TEK	Tie2	tyrosine kinase with Ig-like and EGF-like domains 2	EC marker, angiogenesis [39,40]	GEA00013803
	ACTG2	α-actin	Actin, gamma-enteric smooth muscle	VSMC marker	GEA00025197
	EPHB2	EphB2	Ephrin type-B receptor 2	Arterial EC marker	GEA00029202
	EPHB4	EphB4	Ephrin type-B receptor 4	Venous EC marker, angiogenesis [45]	GEP00059920
Angiogenesis	VEGFA	VEGF-A	Vascular endothelial growth factor	Angiogenesis [40,46,47]	GEA00012311
	TGFB1	TGF-β1	Transforming growth factor beta1	Modulate angiogenesis [34]	GEA00007272
	PCNA	PCNA	Proliferating Cell Nuclear Antigen	Proliferation marker [48]	GEA00012343
	CAT	–	catalase	Oxidative stress & Proliferation [28,49]	GEA00023106
	SGK1	SGK	serum-glucocorticoid-induced protein kinase	Proliferation [50]	GEP00060290
	ANGPT1	–	angiopoietin-1	angiogenesis [40,51]	GEA00013518
	ANGPT2	–	angiopoietin-2	Angiogenesis [52]	GEP00057393
	HIF1A	HIF-1α	Hypoxia-inducible factor 1-alpha	Angiogenesis [53,54]	GEA00012495
	NR4A1	TR3	human orphan receptor TR3	Proliferation [55]	GEA00023496
	ALOX5	5-LO	5-lipoxygenase	Proliferation [56]	GEA00028402
	CD44	–		Proliferation, angiogenesis [57,58]	GEP00056546
	ACE	–	Angiotensin-converting enzyme	Angiogenesis [59]	GEP00058643
Inflammation	IL6	–	Interleukin 6	Inflammation [60]	GEA00012521
	IL8	–	Interleukin 8	Inflammation [61]	GEA00012363
	VCAM1	VCAM-1	vascular cell adhesion molecule 1	Inflammation [32]	GEP00056408
	ICAM1	ICAM-1	Intercellular Adhesion Molecule 1	Inflammation[32]	GEP00056359
	TBXAS1	THA-2	thromboxane synthase-A2	Inflammation [62]	GEP00060291
	NOS3	eNOS	endothelial nitric oxide synthase	Oxidative stress, Inflammation [63,64]	GEA00032450
	CCL2	MCP-1	monocyte chemoattractant protein 1	Inflammation [61,65,66]	GEP00055652
	SELP	–	P-selectin	Adhesion molecular, Inflammation [32]	GEA00030146
	PTGS1	COX-1	Cyclooxygenase-1	Inflammation [67]	GEA00027133
	PTGS2	COX-2	Cyclooxygenase-2	Inflammation [46]	GEA00007158
ECM remodeling	MMP2	MMP-2	matrix metalloproteinase-2	ECM metabolism [22,53,68]	GEA00013719
	MMP9	MMP-9	matrix metalloproteinase-9	ECM metabolism, inflammation [22]	GEA00013721
	MMP14	MMP-14	matrix metalloproteinase-14	ECM metabolism [68]	GEA00026567
	SERPINE1	PAI-1	Plasminogen activator inhibitor-1	ECM metabolism [69,70]	GEP00056400
	TNF	TNF-α	Tumor necrosis factor-α	ECM metabolism, inflammation [68]	GEP00059924
	ITGA7	–	Integrin-α	ECM metabolism [71]	GEP00058254
	TIMP1	TIMP-1	Tissue inhibitor of metalloproteinase 1	ECM metabolism, inflammation [72]	GEA00007289
	TIMP2	TIMP-2	Tissue inhibitor of metalloproteinase 2	ECM metabolism, inflammation [73,74]	GEA00020949
	FN1	–	fibronectin	ECM metabolism [75]	GEA00007778
	TNC	–	Tenasin-C	ECM metabolism [76]	GEA00031358
	SCEL	–	sciellin	ECM metabolism [77]	GEA00031897
	PPL	–	periplakin	ECM metabolism [77]	GEA00032646

[a] Genes used in FACS.
[b] Primer sequences for microfluidic qPCR can be traced by these company assay IDs.

expressed three EC markers CD31, CD34 and CD105, and 30 (22%) expressed four EC markers CD31, CD34, CD105 and CD146. Furthermore, we compared gene expression profiles of EC candidates and LCs. Among the 11 marker genes, eight were differentially expressed between the ECs and LCs (Fig. 3). Among the five marker genes used in FACS, the expression of the LC marker CD45 ($p = 1.2 \times 10^{-27}$) was significantly higher in LCs than ECs, and the expression of EC markers, CD31 ($p = 0.017$), CD34 ($p = 3.1 \times 10^{-5}$) and CD105 ($p = 6.3 \times 10^{-7}$) were significantly higher in the ECs than LCs. The expression of CD146 showed a trend toward higher in ECs than in LCs ($p = 0.15$). In addition, compared to LCs, ECs expressed higher levels of the other four EC specific genes, VEGFR1 ($p = 1.3 \times 10^{-8}$), vWF ($p = 2.3 \times 10^{-7}$), Tie1 ($p = 1.3 \times 10^{-5}$) and THBD ($p = 0.013$). These data indicate that the EC candidates isolated by FACS were indeed ECs.

3.3. Two EC clusters were identified based on gene expression profile

Unsupervised hierarchical clustering separated the 134 ECs into two distinctive clusters according to their expression pattern of the 48 selected functional genes (Fig. 4a). 69 ECs were in cluster A and 65 in cluster B. Principal component analysis (PCA) also showed two distinct populations and was consistent with hierarchical clustering. Only three cluster B cells identified by heat map-based hierarchical clustering were grouped with cluster A cells in PCA, and two cluster A cells were grouped with cluster B cells (Fig. 4b). The correlation of single cell gene expression and different biological donors was also analyzed by PCA. The 2D PCA (Fig. 5a) showed that the ECs from different donors did not overlap and showed no distinguishable cluster. The PCA scree plot (Fig. 5b) showed the contribution of first 10 PCs, which suggested
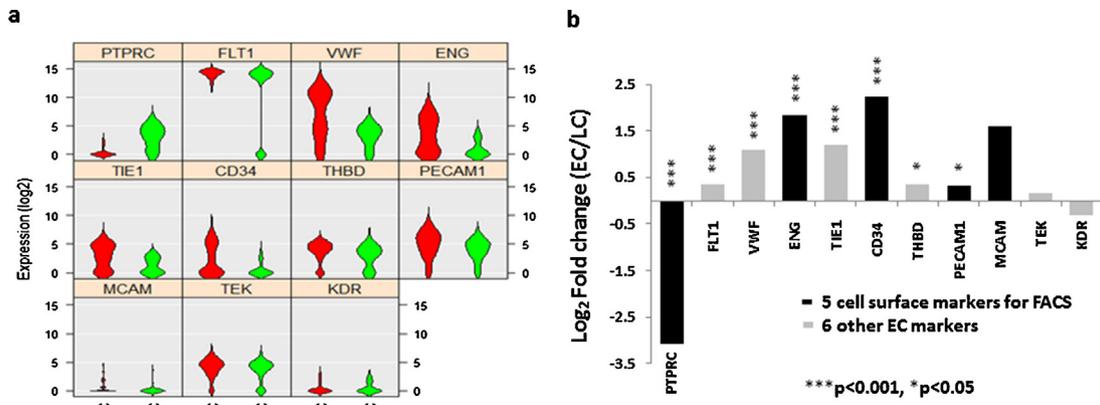
Fig. 3. Differential gene expression of ECs and LCs. (a) Violin plots showed the expression of 11 cell-marker genes are different in the ECs (Red) compared with LCs (Green). The gene name is indicated on top of each violin plot and the value on Y-axle represents the gene expression level in the binary logarithm ($\log_2$) value. (b) Bar graph shows the values of differential gene expression by fold change of the binary logarithm ($\log_2$) in ECs relative to LCs (*$p < 0.05$; ***$p < 0.001$). Gene symbols are used in the figures and corresponding gene names can be found in Table 2. (For interpretation of the references to colour in this figure legend, the reader is referred to the web version of this article.)
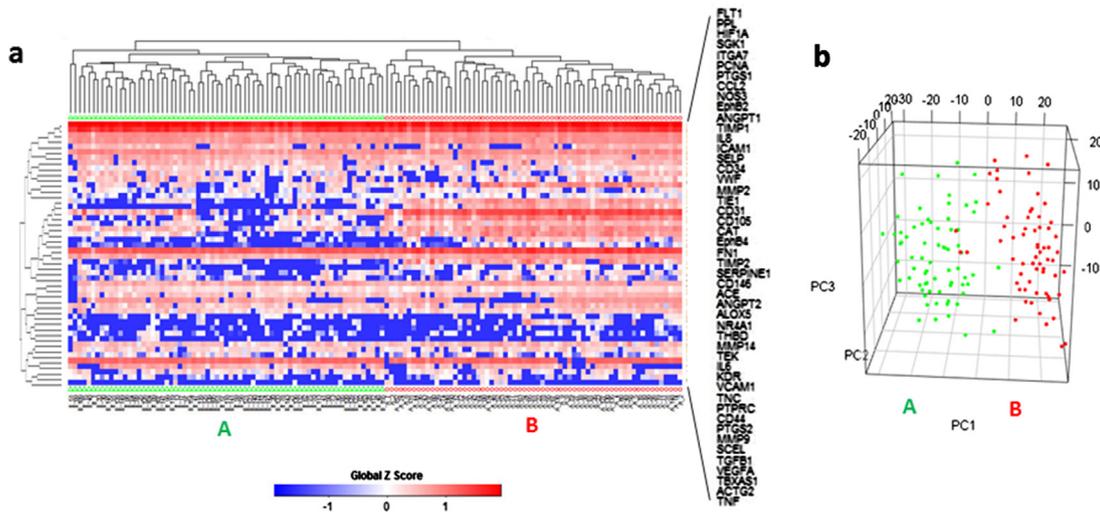

Fig. 4. Two EC clusters were identified by gene expression profiles. (a) Heat map and hierarchical clustering separated the 134 ECs into 2 major clusters, A ($n = 69$, green triangle) and B ($n = 65$, Red circle), based on their expression pattern of the 48 selected genes. (b) 3D PCA plots confirmed the segregation of these two clusters. Cluster A is annotated by green dots and B by Red dots. Gene symbols are used in the figures and corresponding gene names can be found in Table 2. (For interpretation of the references to colour in this figure legend, the reader is referred to the web version of this article.)
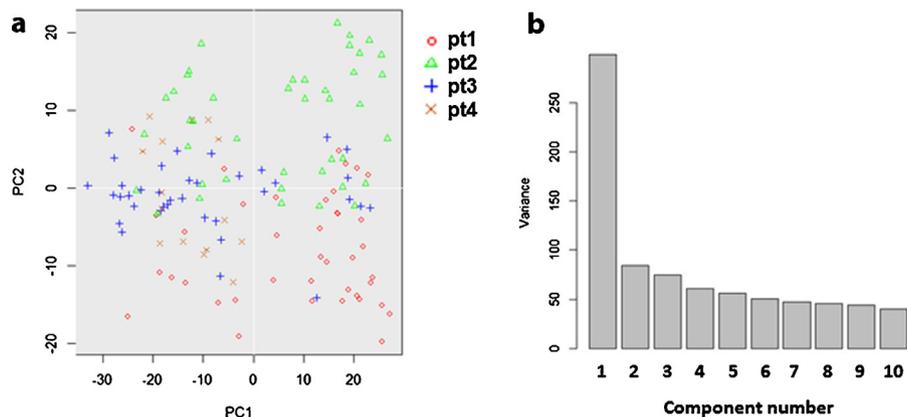

Fig. 5. Two clusters identification is stronger identifiers than donor origin. (a) 2D PCA of the 134 ECs from 4 different donors based on their gene expression profile indicated no clear cluster separation among donors. (b) PCA scree plot of the first 10 PCs suggested the PC1 which identifies the two clusters gives much more contribution to the whole variance than other PCs.

the PC1 which identifies the two clusters gives much more contribution than other PCs.

3.5. Differential gene expression of the 2 EC subsets

Further analysis showed that seven out of the 19 angiogenesis-related genes were differentially expressed (Fig. 6a Left) by cluster A and B. Among them, five were higher in cluster B [vWF ($p = 7.1 \times 10^{-20}$), CD105 ($p = 9.0 \times 10^{-18}$), TIE1 ($p = 1.1 \times 10^{-13}$), CAT ($p = 7.8 \times 10^{-12}$) and EPHB4 ($p = 9.7 \times 10^{-11}$)], two were higher in cluster A [VEGFA ($p = 1.2 \times 10^{-4}$) and TGFB1 ($p = 0.023$)]. Compared to cluster A, cluster B express higher levels of seven out of 13 inflammation-related genes (Fig. 6a Middle), [CD34 ($p = 9.0 \times 10^{-39}$), P-selectin ($p = 9.0 \times 10^{-22}$), CD31 ($p = 1.2 \times 10^{-9}$), CD146 ($p = 3.1 \times 10^{-7}$), VCAM-1 ($p = 1.4 \times 10^{-4}$), COX2 ($p = 0.008$) and ICAM-1 ($p = 0.028$)], as well as five out of the 12 ECM remodeling-related genes, were also expressed higher by cluster B than cluster A cells (Fig. 6a Right), [MMP2 ($p = 5.0 \times 10^{-27}$), PAI-1 ($p = 1.7 \times 10^{-15}$), FN1 ($p = 1.1 \times 10^{-15}$), TIMP1 ($p = 2.9 \times 10^{-11}$) and TIMP2 ($p = 9.5 \times 10^{-6}$)].

4. Discussion

In this study we demonstrated an innovative strategy for analyzing gene expression profiles of ECs collected from vessels on a single cell level. ECs are collected from endovascular guide wires through FACS. Single cell gene expression is analyzed using high throughput microfluidic quantitative RT-PCR. This method could be used to analyze the changes of EC gene expression at single cell level in vascular lesions. A total of 48 genes in four categories (cell-marker, angiogenesis, inflammation and ECM) were analyzed in this study. Two distinctive ECs clusters were identify from ECs collected from normal iliac arteries, suggesting ECs in normal vessel are heterogeneous.

Researchers who study ECs collected using endovascular techniques encounter a paradox that more EC marker genes need to be detected to identify and characterize the collected ECs, while the EC number harvested from such samples is often too small for such multiple marker detection. The traditional assays such as bulk RT-PCR, real-time RT-PCR or quantitative immunocytochemistry can only detect the mRNA transcription or protein expression of up to 3–4 EC functional genes, which are not enough for this purpose. The combination of single EC sorting and high throughput microfluidic quantitative RT-PCR allowed us to check EC identity through analyzing the expression of both the EC specific markers and the expression of functional genes in individual cells simultaneously. Moreover, because this microfluidic quantitative RT-PCR array technology has 96 gene slots, researchers have much more flexibility to expand the functional genes studied to help characterize ECs in varying disease conditions. This technique also presents a sound basis for comparing EC sampling and characterization data from different research centers.

Based on gene expression profiles, two distinctive clusters were identified in ECs collected from normal iliac arteries. A likely
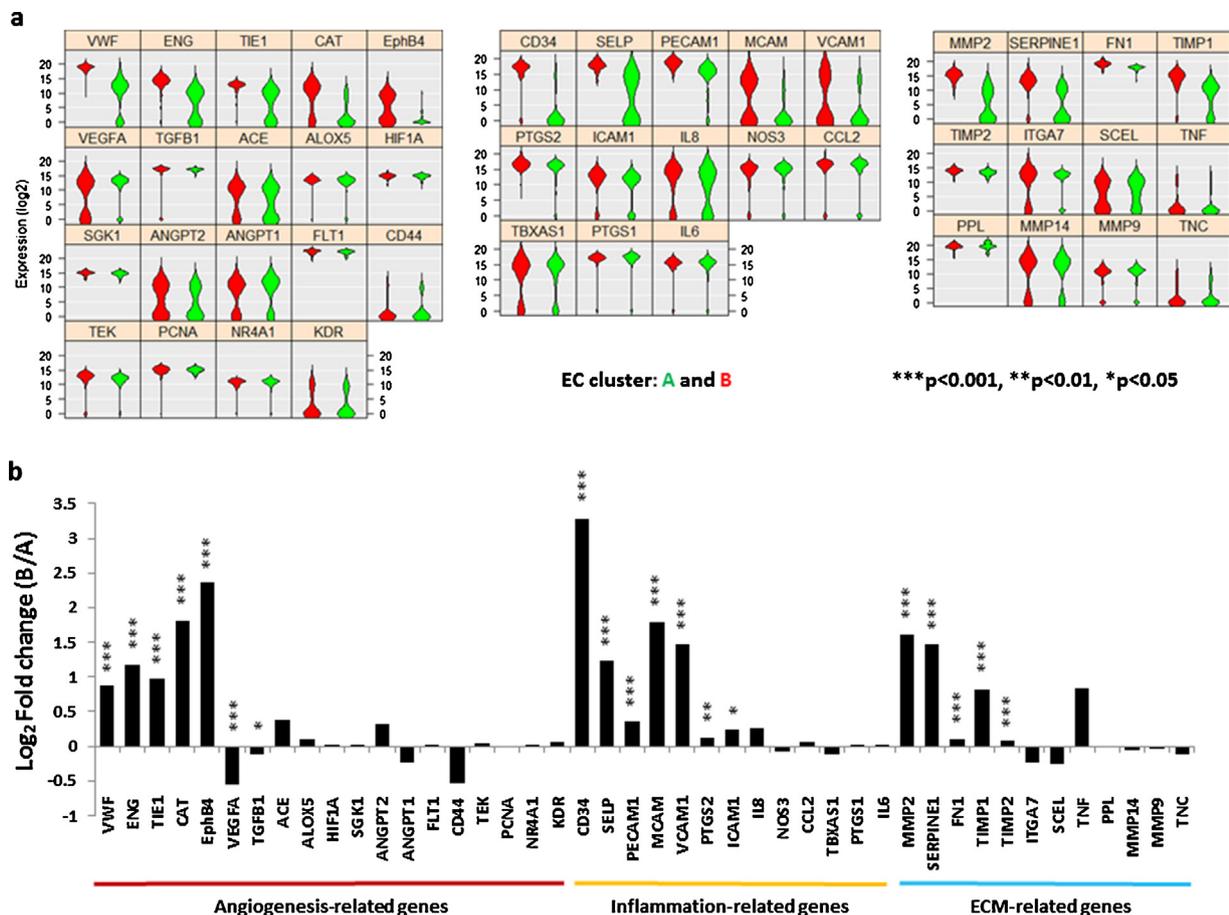

Fig. 6. Differential gene expression of the two EC clusters. (a) Violin plots. Three functional gene groups are included, 19 angiogensis-related genes (Left), 13 inflammation-related genes (Middle) and 12 ECM remodeling genes (Right) of cluster A (green) and cluster B (Red). The gene name is indicated on top of each violin plot and the value on Y-axle represents the gene expression level in the binary logarithm (log_2) value. (b) Bar graph shows the magnitude of differential gene expression by fold change of the binary logarithm (log_2) value in cluster B relative to A (*$p < 0.05$; **$p < 0.01$; ***$p < 0.001$). Gene symbols are used in the figures and corresponding gene names can be found in Table 2. (For interpretation of the references to colour in this figure legend, the reader is referred to the web version of this article.)

explanation is that ECs in normal conditions undergo turnover. The two EC clusters represent ECs at different functional stages, for example healthy and senescent. ECs are a stable cell type with an average turnover rate of about three years [23]. Senescent endothelium has been reported to have decreased expression of angiogenesis and proliferation genes, attenuated production of dilating factors and increased expression of contracting factors, increased oxidative stress, increased production of leukocyte adhesion-related cytokines or inflammation-related cytokines, and increased apoptosis [23]. Although not typical, cluster B ECs showed an expression pattern reminiscent of senescence-related genes like those of previous studies on EC aging and senescence. These gene expression changes include attenuated gene expression of VEGF and TGFβ1 [24], enhanced expression of CD105 (also a EC proliferative marker) [25], COX2 [26,27], catalase [28], VCAM1 and ICAM1 [29], and TIMP2 [30]. Therefore cluster B cells could represent more mature or aged ECs. It is also of interest that cluster B ECs showed enhanced EPHB4 expression compared to cluster A. Although EphB4 is commonly considered a marker for ECs from veins, there is also data indicating EphB4 is expressed on both normal arteries and veins [31]. This gives more supportive evidence that caution should be used when this marker is used to identify venous ECs. We also ran a comparable volume (50ul) blood from each of the same patients on FACS and found no ECs. So, it is unlikely that these ECs came from veins by circulation and attached to the wire.

A noticeable phenomenon in this study is that only a quarter of the FACS sorted ECs expressed the four markers used for sorting and half expressed three. This indicated that FACS sorting cannot give a 100% pure population and a possible solution for this issue is the use of FACs machines with Index sorting capabilities. Several limitations of our study must also be considered. First, the patients selected for cell collection were not matched for their respective diseases necessitating angiography, demographic and co-morbid conditions. Given the small scale and exploratory nature of the study, controlling for such confounders proved difficult. Despite the absence of such analysis, when ECs were analyzed as it related to their patient origin, we noted no significant differences by either PCA or hierarchical clustering. Second, our choice of target genes for microfluidic quantitative RT-PCR was based on literature searches, introducing unavoidable bias. A more objective selection of target genes may be possible by analysis of previous microarray data on ECs. Such analyses are not possible on such small numbers of cells available, though emerging single cell mRNA sequencing may give an unbiased view of the global gene expression and ultimately identify new genes for study. Lastly, EC gene expression profile analysis was based on fewer than 200 ECs from four patients. Further studies of single EC gene expression and transcriptional regulation based on more ECs separated using endovascular cell collection techniques are necessary to investigate differential gene expression in ECs at different vasculature loci and in various vascular lesions.

Sources of funding

Disclosures

None.

Acknowledgements

References

[1] V. Sammons, A. Davidson, J. Tu, M.A. Stoodley, Endothelial cells in the context of brain arteriovenous malformations, J. Clin. Neurosci. 18 (2011) 165–170.

[2] N. Chalouhi, M.S. Ali, P.M. Jabbour, S.I. Tjoumakaris, L.F. Gonzalez, R.H. Rosenwasser, et al., Biology of intracranial aneurysms: role of inflammation, J. Cereb. Blood Flow Metab. 32 (September) (2012) 1659–1676.

[3] U. Landmesser, H. Drexler, The clinical significance of endothelial dysfunction, Curr. Opin. Cardiol. 20 (November) (2005) 547–551.

[4] L. Feng, D.M. Stern, J. Pile-Spellman, Human endothelium: endovascular biopsy and molecular analysis, Radiology 212 (September) (1999) 655–664.

[5] L. Feng, C. Matsumoto, A. Schwartz, A.M. Schmidt, D.M. Stern, J. Pile-Spellman, Chronic vascular inflammation in patients with type 2 diabetes: endothelial biopsy and RT-PCR analysis, Diabetes Care 28 (February) (2005) 379–384.

[6] D. Onat, S. Jelic, A.M. Schmidt, J. Pile-Spellman, S. Homma, M. Padeletti, et al., Vascular endothelial sampling and analysis of gene transcripts: a new quantitative approach to monitor vascular inflammation, J. Appl. Physiol. 103 (2007) 1873–1878.

[7] S.Y. Yu, Y.M. Song, A.M. Li, X.J. Yu, G. Zhao, M.B. Song, et al., Isolation and characterization of human coronary artery-derived endothelial cells in vivo from patients undergoing percutaneous coronary interventions, J. Vasc. Res. 46 (2009) 487–494.

[8] P.C. Colombo, A.W. Ashton, S. Celaj, A. Talreja, J.E. Banchs, N.B. Dubois, et al., Biopsy coupled to quantitative immunofluorescence: a new method to study the human vascular endothelium, J. Appl. Physiol. 92 (March) (2002) 1331–1338.

[9] P.C. Colombo, J.E. Banchs, S. Celaj, A. Talreja, J. Lachmann, S. Malla, et al., Endothelial cell activation in patients with decompensated heart failure, Circulation 111 (January) (2005) 58–62.

[10] I. Eskurza, Z.D. Kahn, D.R. Seals, Xanthine oxidase does not contribute to impaired peripheral conduit artery endothelium-dependent dilatation with ageing, J. Physiol. 571 (March) (2006) 661–668.

[11] P.E. Gates, M.L. Boucher, A.E. Silver, K.D. Monahan, D.R. Seals, Impaired flow-mediated dilation with age is not explained by L-arginine bioavailability or endothelial asymmetric dimethylarginine protein expression, J. Appl. Physiol. 102 (January) (2007) 63–71.

[12] A.E. Silver, S.D. Beske, D.D. Christou, A.J. Donato, K.L. Moreau, I. Eskurza, et al., Overweight and obese humans demonstrate increased vascular endothelial NAD(P)H oxidase-p47(phox) expression and evidence of endothelial oxidative stress, Circulation 115 (February) (2007) 627–637.

[13] A.J. Donato, I. Eskurza, A.E. Silver, A.S. Levy, G.L. Pierce, P.E. Gates, et al., Direct evidence of endothelial oxidative stress with aging in humans: relation to impaired endothelium-dependent dilation and upregulation of nuclear factor-kappaB, Circ. Res. 100 (June) (2007) 1659–1666.

[14] A.E. Silver, D.D. Christou, A.J. Donato, S.D. Beske, K.L. Moreau, K.A. Magerko, et al., Protein expression in vascular endothelial cells obtained from human peripheral arteries and veins, J. Vasc. Res. 47 (2010) 1–8.

[15] D.J. Nolan, M. Ginsberg, E. Israely, B. Palikuqi, M.G. Poulos, D. James, et al., Molecular signatures of tissue-specific microvascular endothelial cell heterogeneity in organ maintenance and regeneration, Dev. Cell. 26 (July) (2013) 204–219.

[16] L.W. Harris, M. Wayland, M. Lan, M. Ryan, T. Giger, H. Lockstone, et al., The cerebral microvasculature in schizophrenia: a laser capture microdissection study, PLoS One 3 (2008) e3964.

[17] Z. Sun, H. Su, B. Long, E. Sinclair, S.W. Hetts, R.T. Higashida, et al., Endothelial cell high-enrichment from endovascular biopsy sample by laser capture microdissection and fluorescence activated cell sorting, J. Biotechnol. 192PA (October) (2014) 34–39.

[18] A.K. White, M. VanInsberghe, O.I. Petriv, M. Hamidi, D. Sikorski, M.A. Marra, et al., High-throughput microfluidic single-cell RT-qPCR, Proc. Natl. Acad. Sci. U.S.A. 108 (August) (2011) 13999–14004.

[19] V. Sanchez-Freire, A.D. Ebert, T. Kalisky, S.R. Quake, J.C. Wu, Microfluidic single-cell real-time PCR for comparative analysis of gene expression patterns, Nat. Protoc. 7 (May) (2012) 829–838.

[20] B.D. MacArthur, A. Sevilla, M. Lenz, F.J. Muller, B.M. Schuldt, A.A. Schuppert, et al., Nanog-dependent feedback loops regulate murine embryonic stem cell heterogeneity, Nat. Cell Biol. 14 (November) (2012) 1139–1147.

[21] S. Lehoux, A. Tedgui, Cellular mechanics and gene expression in blood vessels, J. Biomech. 36 (May) (2003) 631–643.

[22] M.A. Anwar, J. Shalhoub, C.S. Lim, M.S. Gohel, A.H. Davies, The effect of pressure-induced mechanical stretch on vascular wall differential gene expression, J. Vasc. Res. 49 (2012) 463–478.

[23] R.P. Brandes, I. Fleming, R. Busse, Endothelial aging, Cardiovasc. Res. 66 (May) (2005) 286–294.

[24] E. Sadoun, M.J. Reed, Impaired angiogenesis in aging is associated with alterations in vessel density, matrix composition, inflammatory response, and growth factor expression, J. Histochem. Cytochem. 51 (September) (2003) 1119–1130.

[25] F.J. Blanco, M.T. Grande, C. Langa, B. Oujo, S. Velasco, A. Rodriguez-Barbero, et al., S-endoglin expression is induced in senescent endothelial cells and contributes to vascular pathology, Circ. Res. 103 (December) (2008) 1383–1392.

[26] C. Heymes, A. Habib, D. Yang, E. Mathieu, F. Marotte, J. Samuel, et al., Cyclo-oxygenase-1 and -2 contribution to endothelial dysfunction in ageing, Br. J. Pharmacol. 131 (October) (2000) 804–810.

[27] Y. Mukai, H. Shimokawa, T. Higashi, K. Morikawa, T. Matoba, J. Hiroki, et al., Inhibition of renin-angiotensin system ameliorates endothelial dysfunction associated with aging in rats, Arterioscler. Thromb. Vasc. Biol. 22 (September) (2002) 1445–1450.

[28] J. Han, V.V. Shuvaev, V.R. Muzykantov, Catalase and superoxide dismutase conjugated with platelet-endothelial cell adhesion molecule antibody distinctly alleviate abnormal endothelial permeability caused by exogenous reactive oxygen species and vascular endothelial growth factor, J. Pharmacol. Exp. Ther. 338 (July) (2011) 82–91.

[29] N. Morisaki, I. Saito, K. Tamura, J. Tashiro, M. Masuda, T. Kanzaki, et al., New indices of ischemic heart disease and aging: studies on the serum levels of soluble intercellular adhesion molecule-1 (ICAM-1) and soluble vascular cell adhesion molecule-1 (VCAM-1) in patients with hypercholesterolemia and ischemic heart disease, Atherosclerosis 131 (May) (1997) 43–48.

[30] T. Koike, R.B. Vernon, M.D. Gooden, E. Sadoun, M.J. Reed, Inhibited angiogenesis in aging: a role for TIMP-2, J. Gerontol. A Biol. Sci. Med. Sci. 58 (September) (2003) B798–B805.

[31] S. Diehl, R. Bruno, G.A. Wilkinson, D.A. Loose, J. Wilting, L. Schweigerer, et al., Altered expression patterns of EphrinB2 and EphB2 in human umbilical vessels and congenital venous malformations, Pediatr. Res. 57 (April) (2005) 537–544.

[32] C.F. Krieglstein, D.N. Granger, Adhesion molecules and their role in vascular disease, Am. J. Hypertens. 14 (June) (2001) 44S–54S.

[33] J.S. Nielsen, K.M. McNagny, Novel functions of the CD34 family, J. Cell Sci. 121 (November) (2008) 3683–3692.

[34] S. Park, T.A. Dimaio, W. Liu, S. Wang, C.M. Sorenson, N. Sheibani, Endoglin regulates the activation and quiescence of endothelium by participating in canonical and non-canonical TGF-beta signaling pathways, J. Cell Sci. 126 (March) (2013) 1392–1405.

[35] A.N. Solovey, L. Gui, L. Chang, J. Enenstein, P.V. Browne, R.P. Hebbel, Identification and functional assessment of endothelial P1H12, J. Lab. Clin. Med. 138 (November) (2001) 322–331.

[36] A. Kratzer, H.W. Chu, J. Salys, Z. Moumen, M. Leberl, R. Bowler, et al., Endothelial cell adhesion molecule CD146: implications for its role in the pathogenesis of COPD, J. Pathol. 230 (August) (2013) 388–398.

[37] N. Bardin, F. George, M. Mutin, C. Brisson, N. Horschowski, V. Frances, et al., S-Endo 1, a pan-endothelial monoclonal antibody recognizing a novel human endothelial antigen, Tissue Antigens 48 (November) (1996) 531–539.

[38] N. Bardin, D. Reumaux, K. Geboes, J.F. Colombel, M. Blot-Chabaud, J. Sampol, et al., Increased expression of CD146, a new marker of the endothelial junction in active inflammatory bowel disease, Inflamm. Bowel Dis. 12 (January) (2006) 16–21.

[39] W. Zheng, L.P. Christensen, R.J. Tomanek, Stretch induces upregulation of key tyrosine kinase receptors in microvascular endothelial cells, Am. J. Physiol. Heart Circ. Physiol. 287 (December) (2004) H2739–H2745.

[40] S.C. Satchell, K.L. Anderson, P.W. Mathieson, Angiopoietin 1 and vascular endothelial growth factor modulate human glomerular endothelial cell barrier properties, J. Am. Soc. Nephrol. 15 (March) (2004) 566–574.

[41] A. Orecchia, P.M. Lacal, C. Schietroma, V. Morea, G. Zambruno, C.M. Failla, Vascular endothelial growth factor receptor-1 is deposited in the extracellular matrix by endothelial cells and is a ligand for the alpha 5 beta 1 integrin, J. Cell Sci. 116 (September) (2003) 3479–3489.

[42] R.M. Porat, M. Grunewald, A. Globerman, A. Itin, G. Barshtein, L. Alhonen, et al., Specific induction of tie1 promoter by disturbed flow in atherosclerosis-prone vascular niches and flow-obstructing pathologies, Circ. Res. 94 (February) (2004) 394–401.

[43] F.A. Martin, R.P. Murphy, P.M. Cummins, Thrombomodulin and the vascular endothelium: insights into functional, regulatory, and therapeutic aspects, Am. J. Physiol. Heart Circ. Physiol. 304 (June) (2013) H1585–H1597.

[44] A.M. Randi, M.A. Laffan, R.D. Starke, Von Willebrand factor, angiodysplasia and angiogenesis, Mediterr. J. Hematol. Infect. Dis. 5 (2013) e2013060.

[45] C. Yang, Y. Guo, C.C. Jadlowiec, X. Li, W. Lv, L.S. Model, et al., Vascular endothelial growth factor-A inhibits EphB4 and stimulates delta-like ligand 4 expression in adult endothelial cells, J. Surg. Res. 183 (July) (2013) 478–486.

[46] P.C. Akarasereenont, K. Techatraisak, A. Thaworn, S. Chotewuttakorn, The expression of COX-2 in VEGF-treated endothelial cells is mediated through protein tyrosine kinase, Mediators Inflamm. 11 (February) (2002) 17–22.

[47] E. Sho, M. Komatsu, M. Sho, H. Nanjo, T.M. Singh, C. Xu, et al., High flow drives vascular endothelial cell proliferation during flow-induced arterial remodeling associated with the expression of vascular endothelial growth factor, Exp. Mol. Pathol. 75 (August) (2003) 1–11.

[48] N.E. Hurley, L.A. Schildmeyer, K.A. Bosworth, Y. Sakurai, S.G. Eskin, L.H. Hurley, et al., Modulating the functional contributions of c-Myc to the human endothelial cell cyclic strain response, J. Vasc. Res. 47 (2010) 80–90.

[49] S.R. Frye, A. Yee, S.G. Eskin, R. Guerra, X. Cong, L.V. McIntire, cDNA microarray analysis of endothelial cells subjected to cyclic mechanical strain: importance of motion control, Physiol. Genomics 21 (March) (2005) 124–130.

[50] F. Ferrelli, D. Pastore, B. Capuani, M.F. Lombardo, M. Blot-Chabaud, A. Coppola, et al., Serum glucocorticoid inducible kinase (SGK)-1 protects endothelial cells against oxidative stress and apoptosis induced by hyperglycaemia, Acta Diabetol. (June) (2014) 55–64.

[51] I. Kim, H.G. Kim, J.N. So, J.H. Kim, H.J. Kwak, G.Y. Koh, Angiopoietin-1 regulates endothelial cell survival through the phosphatidylinositol 3′-Kinase/Akt signal transduction pathway, Circ. Res. 86 (January) (2000) 24–29.

[52] C. Daly, E. Pasnikowski, E. Burova, V. Wong, T.H. Aldrich, J. Griffiths, et al., Angiopoietin-2 functions as an autocrine protective factor in stressed endothelial cells, Proc. Natl. Acad. Sci. U.S.A. 103 (October) (2006) 15491–15496.

[53] M. Milkiewicz, T.L. Haas, Effect of mechanical stretch on HIF-1li and MMP-2 expression in capillaries isolated from overloaded skeletal muscles: laser capture microdissection study, Am. J. Physiol. Heart Circ. Physiol. 289 (September) (2005) H1315–20.

[54] M. Milkiewicz, J.L. Doyle, T. Fudalewski, E. Ispanovic, M. Aghasi, T.L. Haas, HIF-1alpha and HIF-2alpha play a central role in stretch-induced but not shear-stress-induced angiogenesis in rat skeletal muscle, J. Physiol. 583 (September) (2007) 753–766.

[55] E.K. Arkenbout, M. van Bragt, E. Eldering, C. van Bree, J.M. Grimbergen, P.H. Quax, et al., TR3 orphan receptor is expressed in vascular endothelial cells and mediates cell cycle arrest, Arterioscler. Thromb. Vasc. Biol. 23 (September) (2003) 1535–1540.

[56] J.L. Walker, J. Loscalzo, Y.Y. Zhang, 5-Lipoxygenase and human pulmonary artery endothelial cell proliferation, Am. J. Physiol. Heart Circ. Physiol. 282 (February) (2002) H585–H593.

[57] V. Trochon, C. Mabilat, P. Bertrand, Y. Legrand, F. Smadja-Joffe, C. Soria, et al., Evidence of involvement of CD44 in endothelial cell proliferation, migration and angiogenesis in vitro, Int. J. Cancer 66 (May) (1996) 664–668.

[58] M. Tsuneki, J.A. Madri, CD44 regulation of endothelial cell proliferation and apoptosis via modulation of CD31 and VE-cadherin expression, J. Biol. Chem. 289 (February) (2014) 5357–5370.

[59] E.A. Silva, C. Eseonu, D.J. Mooney, Endothelial cells expressing low levels of CD143 (ACE) exhibit enhanced sprouting and potency in relieving tissue ischemia, Angiogenesis 17 (July) (2014) 617–630.

[60] S. Kobayashi, M. Nagino, S. Komatsu, K. Naruse, Y. Nimura, M. Nakanishi, et al., Stretch-induced IL-6 secretion from endothelial cells requires NF-kappaB activation, Biochem. Biophys. Res. Commun. 308 (August) (2003) 306–312.

[61] M. Okada, A. Matsumori, K. Ono, Y. Furukawa, T. Shioi, A. Iwasaki, et al., Cyclic stretch upregulates production of interleukin-8 and monocyte chemotactic and activating factor/monocyte chemoattractant protein-1 in human endothelial cells, Arterioscler. Thromb. Vasc. Biol. 18 (June) (1998) 894–901.

[62] H. Zhao, T. Hiroi, B.S. Hansen, J.J. Rade, Cyclic stretch induces cyclooxygenase-2 gene expression in vascular endothelial cells via activation of nuclear factor kappa-beta, Biochem. Biophys. Res. Commun. 389 (November) (2009) 599–601.

[63] H. Matsushita, E. Chang, A.J. Glassford, J.P. Cooke, C.P. Chiu, P.S. Tsao, eNOS activity is reduced in senescent human endothelial cells: preservation by hTERT immortalization, Circ. Res. 89 (October) (2001) 793–798.

[64] J. Hoffmann, J. Haendeler, A. Aicher, L. Rossig, M. Vasa, A.M. Zeiher, et al., Aging enhances the sensitivity of endothelial cells toward apoptotic stimuli: important role of nitric oxide, Circ. Res. 89 (October) (2001) 709–715.

[65] B.S. Wung, J.J. Cheng, H.J. Hsieh, Y.J. Shyy, D.L. Wang, Cyclic strain-induced monocyte chemotactic protein-1 gene expression in endothelial cells involves reactive oxygen species activation of activator protein 1, Circ. Res. 81 (July) (1997) 1–7.

[66] B.S. Wung, J.J. Cheng, S.K. Shyue, D.L. Wang, NO modulates monocyte chemotactic protein-1 expression in endothelial cells under cyclic strain, Arterioscler. Thromb. Vasc. Biol. 21 (December) (2001) 1941–1947.

[67] A. Tailor, K.C. Wood, J.L. Wallace, R.D. Specian, D.N. Granger, Roles of platelet and endothelial cell COX-1 in hypercholesterolemia-induced microvascular dysfunction, Am. J. Physiol. Heart Circ. Physiol. 293 (December) (2007) H3636–42.

[68] B.W. Wang, H. Chang, S. Lin, P. Kuan, K.G. Shyu, Induction of matrix metalloproteinases-14 and -2 by cyclical mechanical stretch is mediated by tumor necrosis factor-alpha in cultured human umbilical vein endothelial cells, Cardiovasc. Res. 59 (August) (2003) 460–469.

[69] U. Cavallaro, V. Castelli, U. Del Monte, M.R. Soria, Phenotypic alterations in senescent large-vessel and microvascular endothelial cells, Mol. Cell Biol. Res. Commun. 4 (August) (2000) 117–121.

[70] K.E. Foreman, J. Tang, Molecular mechanisms of replicative senescence in endothelial cells, Exp. Gerontol. 38 (November–December) (2003) 1251–1257.

[71] B. Gao, T.M. Saba, M.F. Tsan, Role of alpha(v) beta(3)-integrin in TNF-alpha-induced endothelial cell migration, Am. J. Physiol. Cell Physiol. 283 (October) (2002) C1196–205.

[72] R. Forough, N. Koyama, D. Hasenstab, H. Lea, M. Clowes, S.T. Nikkari, et al., Overexpression of tissue inhibitor of matrix metalloproteinase-1 inhibits vascular smooth muscle cell functions in vitro and in vivo, Circ. Res. 79 (October) (1996) 812–820.

[73] W.B. Saunders, B.L. Bohnsack, J.B. Faske, N.J. Anthis, K.J. Bayless, K.K. Hirschi, et al., Coregulation of vascular tube stabilization by endothelial cell TIMP-2 and pericyte TIMP-3, J. Cell. Biol. 175 (October) (2006) 179–191.

[74] W.G. Stetler-Stevenson, D.W. Seo, TIMP-2: an endogenous inhibitor of angiogenesis, Trends Mol. Med. 11 (March) (2005) 97–103.

[75] T. Kumazaki, Modulation of gene expression during aging of human vascular endothelial cells, Hiroshima J. Med. Sci. 42 (June) (1993) 97–100.

[76] T.R. Alves, A.C. da Fonseca, S.S. Nunes, A.O. da Silva, L.G. Dubois, J. Faria, et al., Tenascin-C in the extracellular matrix promotes the selection of highly proliferative and tubulogenesis-defective endothelial cells, Exp. Cell Res. 317 (September) (2011) 2073–2085.

[77] A.L. Pyle, B. Li, A.B. Maupin, R.J. Guzman, D.L. Crimmins, S. Olson, et al., Biomechanical stress induces novel arterial intima-enriched genes: implications for vascular adaptation to stress, Cardiovasc. Pathol. 19 (March–April) (2010) e13–e20.